IEEE Access
Multidisciplinary | Rapid Review | Open Access Journal

Received September 7, 2018, accepted September 22, 2018, date of publication October 1, 2018, date of current version October 25, 2018.

Digital Object Identifier 10.1109/ACCESS.2018.2872692

A Wideband Single-Fed, Circularly-Polarized Patch Antenna With Enhanced Axial Ratio Bandwidth for UHF RFID Reader Applications

JUNLONG LI[1], HUI LIU[1,2], SHUAI ZHANG[3], MIAOHUI LUO[1], YUAN ZHANG[1], AND SAILING HE[1,2,4], (Fellow, IEEE)

[1]Centre for Optical and Electromagnetic Research, South China Academy of Advanced Optoelectronics, South China Normal University, Guangzhou 510006, China
[2]Center for Optical and Electromagnetic Research, Zhejiang University, Hangzhou 310027, China
[3]Department of Electronic Systems, The Antennas, Propagation and Millimeter-wave Systems Section, Aalborg University, 9220 Aalborg, Denmark
[4]Department of Electromagnetic Engineering, School of Electrical Engineering, KTH Royal Institute of Technology, S-100 44 Stockholm, Sweden

Corresponding author: Sailing He (sailing@kth.se)

This work was supported in part by the National Natural Science Foundation of China under Grant 11621101 and Grant 61108022, in part by the Guangdong Innovative Research Team Program under Grant 201001D0104799318, and in part by the National High Technology Research and Development Program (863 Program) of China under Grant 2012AA030402.

ABSTRACT A wideband single-fed, circularly-polarized patch antenna with enhanced axial ratio bandwidth for RFID reader application is proposed. The antenna consists of a modified half E-shaped patch, a near-field resonant parasitic (NFRP) patch, and four rotated vertical metallic plates on the ground plane. The metallic plates surrounding the main radiator of the modified half E-shaped patch antenna are fabricated vertically on the ground plane. The operating frequency of the antenna decreases substantially with the vertical metallic plates, which is important for miniaturization of RFID applications. With an elliptical slot and a cut on the modified half E-shaped patch, antenna impedance bandwidth and CP performance both improve. A truncated corner patch as an NFRP element can generate an additional CP radiation mode and further enhances the axial ratio and impedance bandwidth. The measured results show that the antenna has an impedance bandwidth of 14.2% (833–960 MHz), a 3-dB AR bandwidth of 9.0% (846–926 MHz), and an average gain of 7.3 dBic over a 3-dB AR bandwidth. The proposed antenna has a compact size and a low profile ($0.45\lambda_0 \times 0.45\lambda_0 \times 0.074\lambda_0$).

INDEX TERMS Compact, low profile, vertical rotated metallic plate, modified half E-shaped patch antenna, circular polarization, UHF radio frequency identification.

I. INTRODUCTION

Circularly-polarized (CP) antennas have been widely applied in modern communication systems, such as radio frequency identifications (RFID), radar, and satellite navigations systems, due to their decreased multipath distortion and ability to avoid polarization mismatching between the transmitting and receiving antennas. Additionally, CP antennas with compact and low-profile structures are necessary for modern compact and lightweight radio equipment.

For lightweight, compact configuration and ease of integration, microstrip patch antennas are frequently designed to generate CP radiation performance. CP radiation can be generated by two orthogonal modes of equal magnitude and a 90° phase offset in space [1], [2]. Two types of patch antennas for generating CP radiation have been presented in previous literature: a multi-fed version [2]–[8] and a single-fed version [9]–[26]. Multi-fed CP patch antennas have the advantages of broad impedance and CP bandwidths [2]–[8]. However, multi-fed CP antennas require bulky volumes or complex structures. Single-fed circularly-polarized microstrip patch antennas have drawn much attention because of their advantages of relatively low manufacturing cost, simple configuration, and compact structures compared to dual-fed and multi-fed types. Nevertheless, most single-fed circularly-polarized patch antennas have a very narrow CP bandwidth, which limits their applications for wideband communication systems [9]–[13], [29].

In order to meet broader circular polarization applications, new single-fed CP antennas are proposed in open literature. A single layer circularly-polarized patch antenna can achieve

good impedance and CP bandwidth with an L-shaped ground plane. By introducing a slit on a direct feeding single-layer, corner-truncated square patch antenna with an L-shaped ground plane, the AR bandwidth of the antenna increases more than 16% [14]. The notched circular patch antenna with L-shaped ground plane can give wide CP bandwidth by loading a parasitic element [15], [16]. However, the antennas in [14]–[16] require a large L-shaped ground plane and also have large sizes. A coupled feeding probe technique improves the impedance matching and CP bandwidth in circularly-polarized patch antennas [17], [18]. However, this results in a larger antenna height, and it is also difficult to assemble the L-shaped feeding probe.

A stacked structure is a promising method to improve the CP bandwidth. A wide operating bandwidth of antenna can be achieved by appropriately stacking multiple radiators of adjacent resonant frequencies [19]–[23]. A wideband CP, multilayered hexagonal microstrip antenna was reported for Global Positioning Systems, consisting of two different sized hexagonal stacked patches with two asymmetric rectangular slots (the lower patch was fed by a microstrip feed line) [19]. A wideband single-fed CP stacked slotted microstrip patch antenna was presented in [20], where the circularly-polarized performance can be generated by using an upper and a lower square asymmetric slotted patch. A square ring antenna was stacked over a square slot ring to generate CP waves by adding four branched slots [21]. A method of stacking a square patch in a square ring antenna was presented to enhance the axial-ratio bandwidth of circularly-polarized (CP) microstrip patch antennas [22], [23]. Furthermore, some new feeding technologies were further utilized to enhance the bandwidth of stacked antenna [24]–[26]. In [24], a circularly polarized stacked electromagnetically coupled patch antenna and its subarray at X band were presented, and the performance of subarray could be improved by using a sequential feeding technique. A H-shaped patch antenna with a wide operational bandwidth for circular polarization was presented in [25], which was singly fed by a long probe in conjunction with a printed monopole. A stacked structure improves the impedance matching and AR bandwidths with a horizontally-meandered strip feeding technique [26]. Even though the CP bandwidth of these stacked antennas is enhanced, they are still somewhat large.

The CP patch antenna is commonly used as a RFID reader antenna to avoid polarization mismatch between the readers and the tags. The frequencies for UHF RFID applications are different in different countries and regions. For example, the frequencies for UHF RFID applications are 840.5–844.5 MHz and 920.5–924.5 MHz in China, 866–869 MHz in Europe, 852–855 MHz, 950–956 MHz in Japan, 865–867 MHz in India, 920–926 MHz in Australia, 908.5–914 MHz in Korea, 902–928 MHz in North America [9]. The RFID tags may operate in different bands. For example, in [27] the operating bandwidth (VSWR$<$5.8) of the tag antenna on a metallic surface was 909–916.5 MHz. The tag antenna in [28] has an operating bandwidth from 848 to 926 MHz. A UHF RFID reader antenna with a wider bandwidth would be beneficial to RFID system configuration and cost reduction and flexibility (work anywhere). Furthermore, a compact and low profile configuration of reader antenna is vital for a space-constrained RFID system.

In this paper, a compact wideband single-fed CP patch antenna with enhanced axial ratio bandwidth for fixed UHF RFID reader applications covering UHF RFID band of 850-925MHz is proposed. The proposed antenna consists of a modified half E-shaped patch, a near-field resonant parasitic (NFRP) patch, and four vertical coupled rotated metallic plates on the ground plane. At the same time, an elliptical slot and a corner cut are etched on the modified half E-shape patch. The modified half E-shaped patch on the top substrate is used as the main radiator in this antenna. Four sequentially rotated metallic plates are vertically placed on the edge of the ground plane, which is utilized to reduce the overall dimensions of the antenna. The elliptical slot and corner cut on the modified half E-shaped patch improve the impedance and CP performance. The near-field resonant parasitic (NFRP) patch is introduced to generate a new pair of orthogonal near-degenerate resonant modes that produce an additional CP radiation mode and broaden the impedance bandwidth by playing directly below the modified half E-shaped radiation patch. Different from the traditional circularly polarized modified half E-shaped patch antenna [29], the antenna achieves wide CP bandwidth of 9.0% after introduction of the NFRP patch. Although the CP bandwidth of traditional circularly-polarized microstrip patch antennas can also be enhanced by the additional the vertical metallic plates, the profile of the antenna is dramatically increased [30]. In the proposed antenna, the dimensions of the antenna can be reduced by the introduction of four rotated vertical metallic plates, while the CP bandwidth is improved without increasing the height of the antenna. The antenna structure is presented in Section II. The design process and parameter study are presented in Section III. Results and analyses are presented in Section IV. Conclusions are given in Section V.

II. ANTENNA GEOMETRY

Configurations of the proposed antenna, which consists of three simple elements: a modified half E-shaped patch, a corner truncated square patch, and four rotated metallic plates on the edge of the ground plane, are illustrated in Fig.1. In Fig.1(a) and (b), the modified half E-shaped patch (main radiation patch) is fabricated on the surface on the top substrate, while a corner truncated square patch is printed on the top of the bottom FR4 substrate. The center probe of an SMA connector threading the bottom substrate is connected to the modified half E-shaped patch antenna perpendicularly. In addition, four metallic plates with a height of h_{n} are placed vertically on the edges of the ground plane, forming a cavity reflector with four gaps to reduce the size of the antenna. The top FR4 substrate is placed above the bottom FR4 substrate at a height of $h_2 = 8$mm, and the bottom FR4 substrate is suspended above the ground plane at a height

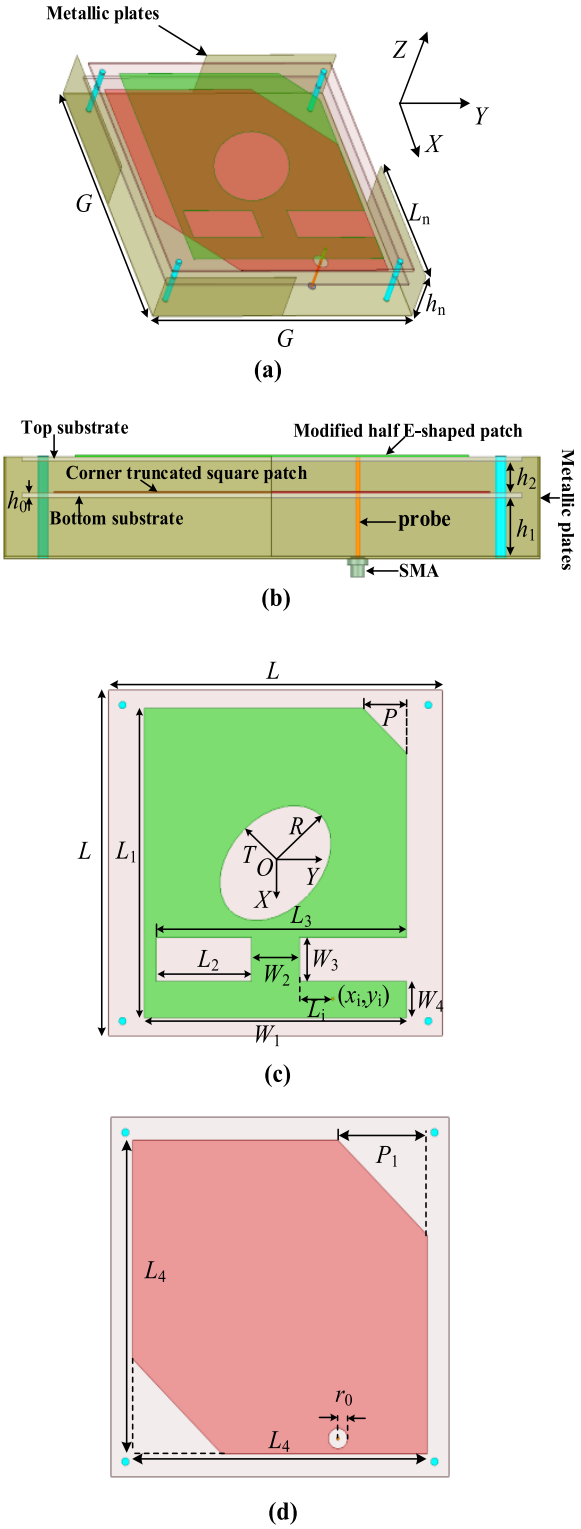

FIGURE 1. Configurations of the proposed antenna.

of $h_1 = 15$mm. All FR4 substrates have a thickness $h_0 = 1$ mm, dielectric constant $\varepsilon_r = 4.4$, and loss tangent $\tan\delta = 0.02$, with dimensions of $L \times L$. Fig. 1(c) shows the details of the modified half E-shaped patch. It can be seen that an elliptical slot and a corner cut are etched on the modified half E-shaped patch. There is a 45° angle between the long axis of the ellipse slot and the y-axis. The long axis of the elliptical slot is R, and the ratio (short axis/long axis) is T. A corner cut with length p is etched in the upper right corner of the modified half E-shaped patch. In Fig.1 (d), a corner truncated patch is printed on top of the bottom substrate as the NFRP patch. A circular slot with a radius r_0 is etched on the NFRP patch for cutting off contact of the corner truncated square patch and the feed probe. The detailed dimensions of the proposed antenna are summarized in Table1.

TABLE 1. Dimension of the proposed antenna.

Symbol	Value(mm)	Symbol	Value(mm)
G	150	P	27
L	140	P_1	30
L_1	125	h_0	1
L_2	40	h_1	15
L_3	105	h_2	8
L_4	122	h_n	25
L_i	14	r_0	4
L_n	75	R	27
W_1	110	T	0.7
W_2	20	x_i	55
W_3	18	y_i	24
W_4	14.5		

III. ANTENNA ANALYSIS AND DESIGN PROCEDURE

A. DESIGN PROCEDURE

To illustrate the design procedure of the proposed antenna, four antennas are modeled and simulated by ANSYS HFSS, as shown in Figure 2. Fig. 3 shows the reflection coefficients and axial ratios of the four antennas. Firstly, we investigate a modified half E-shaped patch antenna without the NFRP patch and four vertical metallic plates, Ant 1. The detailed design process of Ant.1 is similar to that in [29]. According to [29], the half E-shaped patch antenna with a shorting bar can generate circularly-polarized radiation, which has broader impedance bandwidth with a smaller size. For Ant 1, circularly-polarized radiation is achieved by adjusting current magnitudes and phase between the x and y components. It can be observed that two resonant modes are excited, at 950MHz and 1070MHz, in Ant.1. In order to decrease the operating frequency of Ant.1, the dimensions should be enlarged. To retain a compact structure, four rotated vertical metallic plates surrounding the modified half E-shaped patch are introduced on the edges of the ground plane in Ant.2. Due to strengthened coupling between the modified half E-shaped patch and the four rotated vertical metallic plates, the two resonant frequencies are shifted from 950MHz to 855 MHz and from 1070MHz to 980MHz. This indicates that the equivalent resonant length of the antenna can be reduced

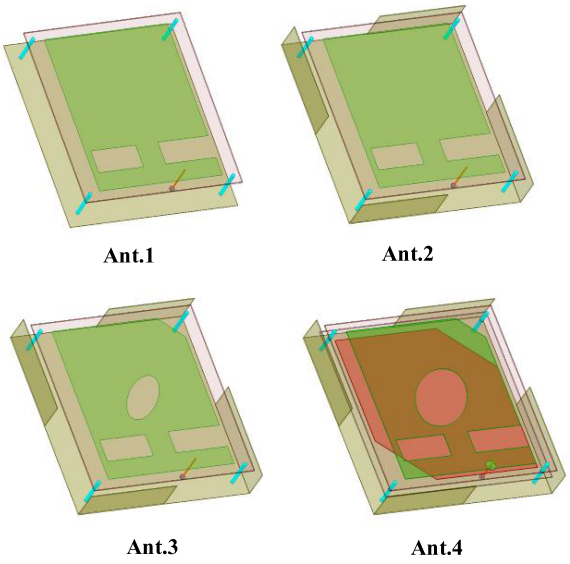

FIGURE 2. Design procedure.

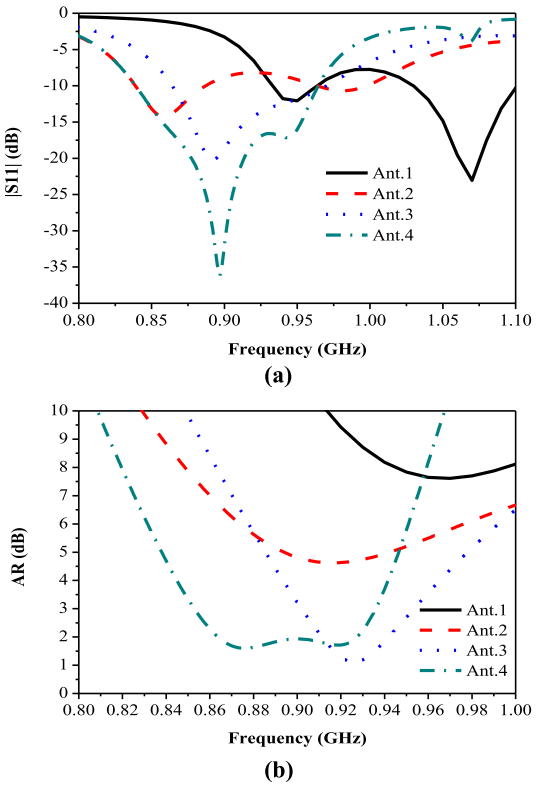

FIGURE 3. Comparison of different antennas: (a) reflection coefficients, (b) AR.

by approximately 10%. Although the resonant frequency of the antenna is reduced by the introduction of the four vertical rotated metallic plates, the impedance matching of Ant.2 is still very poor, and the axial ratio is larger than 3dB in the operating band. To improve the impedance matching and CP performance, an elliptical slot and a corner cut are etched on the modified half E-shaped patch in Ant.3. In [31],

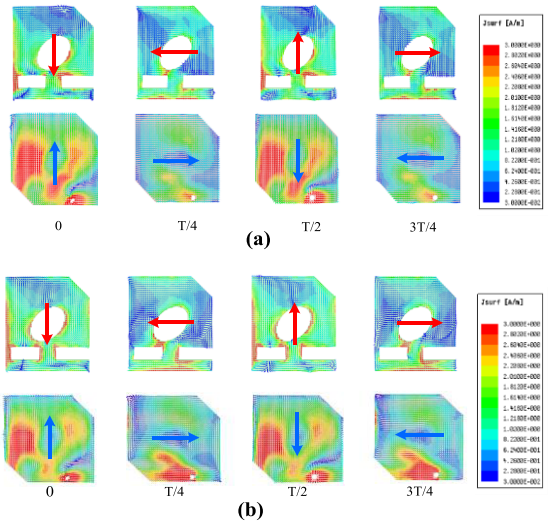

FIGURE 4. Current distributions on the surfaces of the main radiation patch and NFRP patch over one period at (a) 870MHz and (b) 920MHz.

the introduction of the elliptical slot efficiently improves the antenna impedance and the AR performance at operating frequencies. The resonant modes of Ant.3 are shifted close to each other by etching an elliptical slot and a corner cut on the modified half E-shaped patch so that the impedance and AR bandwidth are improved. After parameter optimization for Ant.3, an impedance bandwidth of 11.6% (864MHz-970Mhz) and 3-dB AR bandwidth of 5.6% (902MHz-954MHz) are achieved. To further enhance the impedance and CP bandwidth, a corner truncated square patch directly beneath modified half E-shaped patch is introduced in Ant.4 as a near-field resonant parasitic element. According to [32], the NFRP patch can excite a new pair of orthogonal near-degenerate resonant modes that give rise to an additional CP radiation mode and broaden the impedance bandwidth. As shown in Fig3(b), the NFRP patch in Ant.4 can generate another CP radiation mode and enlarge impedance bandwidth dramatically. It should be noted that the configurations of the NFRP element are different from the main radiation patch. Mutual coupling between the two patches, the elliptical slot, and a corner cut on the main patch allow for further optimization of the overall impedance and CP performance. Finally, a circular slot with a radius r_0 is etched on the NFRP patch to cut off contact with the NRFP patch and SMA probe. After parametric optimization, the impedance bandwidth of Ant.4 is further broadened to 839-964MHz (13.9%). Ant.4 has a wide AR bandwidth of 853-936MHz (9.3%), which is almost the twice as wide as the CP bandwidth of a traditional corner truncated patch antenna without adding four metallic plates (4%) [30].

To investigate the operational mechanisms of the proposed antenna, the current distribution on the surface of the main radiation patch and the NFRP element at 870MHz and 920MHz are plotted in Fig.4 for different time phases: t=0 (0°), T/4 (90°), T/2 (180°), and 3T/4 (270°), where T represents a period. It is observed that the currents on both patches

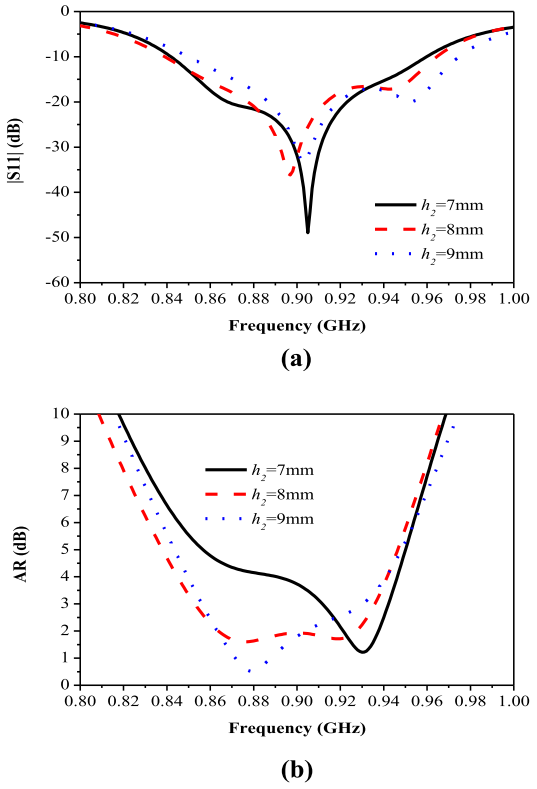

FIGURE 5. Simulated antenna performance with different h_2: (a) reflection coefficients, (b) AR.

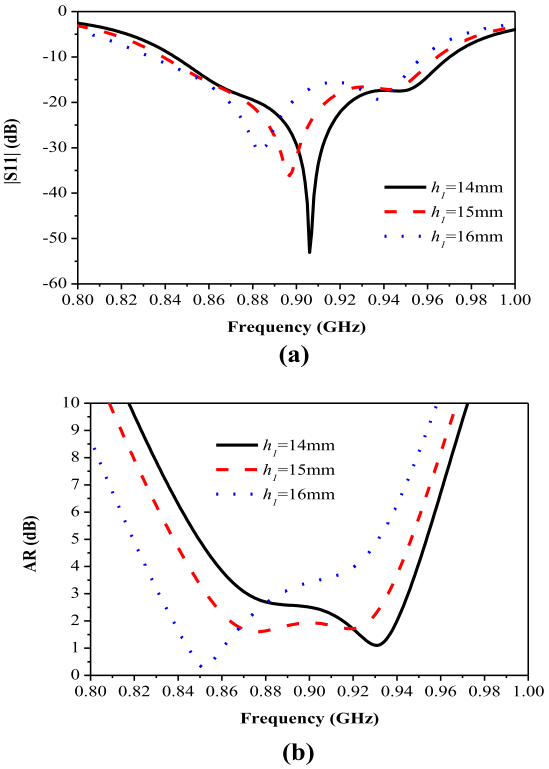

FIGURE 6. Simulated antenna performance with different h1: (a) reflection coefficients, (b) AR.

flow in the clockwise direction as t increases, which produces left-hand circularly polarized (LHCP) radiation. The surface current's effective directions on the main radiation patch and NFRP patch are illustrated with an arrow.

The design procedure is summarized as follows:

(I) The compact modified half E-shaped patch antenna is designed for the desired frequency by the introduction of four rotated metallic plates on the ground plane. The detailed design process of the modified half E-shaped patch antenna is similar to that in [29].

(II) An elliptical slot and the corner cut etching on the modified half E-shaped patch is used to improve the impedance and AR bandwidth of the modified half E-shaped patch antenna with four vertical metallic plates.

(III) The NFRP patch beneath the main radiator excites a new pair of orthogonal near-degenerate resonant modes that produce an additional CP radiation mode and broaden the impedance bandwidth efficiently. The elliptical slot and a corner cut on the main patch allow further optimization of overall impedance and CP bandwidth.

B. PARAMETRIC STUDY

From the above design process, the modified half E-shaped patch and NFRP patch have generated two independent CP modes. Hence, combining them together could improve the impedance and the axial ratio (AR) distinctly, but this will rely on the coupling between both patches and the current perturbation on each patch. Therefore, important parameters of the proposed antenna that can affect performance are studied. Firstly, we investigated the optimal distance between the main radiation patches and the NFRP patch, as well as the height between the NFRP patch and the ground plane. When each parameter is studied, the others are held constant. Fig.5 shows the reflection coefficients and AR for different h_2. As h_2 increases from 7mm to 9mm, the resonant mode in the upper band shifts to a higher frequency. This leads to improved impedance bandwidth, but the AR performance is degraded greatly at the higher frequency. When the parameter h_2 is set to 8 mm, a broader AR bandwidth is obtained. There is a trade-off between the impedance and AR bandwidth. Fig.6 shows the results for different heights h_1. As h_1 increases from 14mm to 16 mm, the resonant mode in the low band shift to a lower frequency, but the AR deteriorate in the upper band. These results illustrate that the impedance and AR bandwidth are highly affected by h_1 and h_2. Furthermore, tuning h_1 and h_2 can improve the AR bandwidth and impedance matching in the operating band.

Next, the sizes of the elliptical slot and the corner cuts on the modified half E-shaped patch are investigated in the proposed antenna. The studied parameters of the elliptical slot on the main radiation patch are the long axis (R) and the ratio between the axes (T). Fig. 7 shows the impedance and AR bandwidth with different R and T. AR bandwidth is greatly improved as R increases from 26 to 27 mm and as T increases from 0.6 to 0.7. However, the CP performance diminishes when R is 28 mm and T is 0.8. The influence

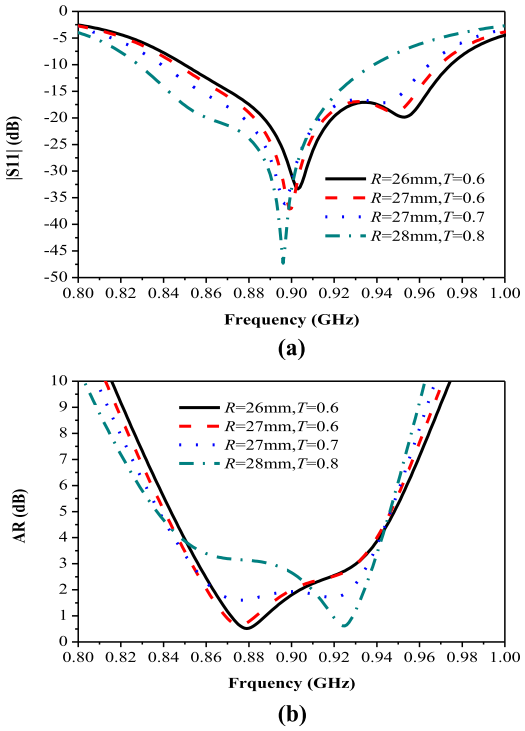

FIGURE 7. Simulated antenna performance with different R,T: (a) reflection coefficients, (b) AR.

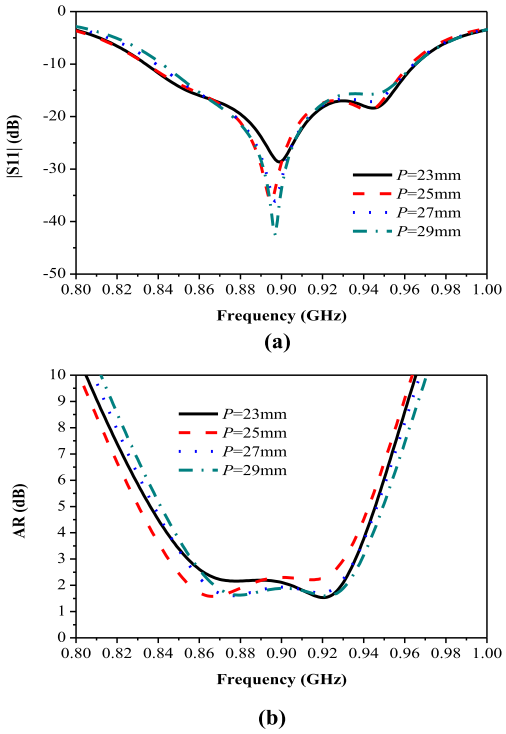

FIGURE 8. Simulated antenna performance with different P: (a) reflection coefficients, (b) AR.

of corner cut length P on the antenna is shown in Fig. 8. It can be seen that adjusting P can improve the AR bandwidth while negligibly impacting the impedance bandwidth.

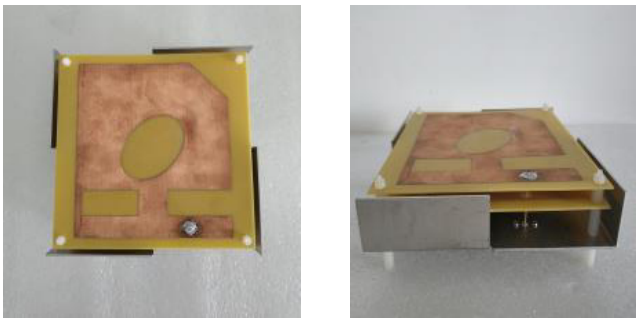

FIGURE 9. Fabricated prototype of the proposed circularly polarized antenna. (a) Top view. (b) Side view.

Therefore, we use the appropriate sizes of the elliptical slot and the corner cuts to optimize CP characteristics of the proposed antenna.

IV. EXPERIMENTAL RESULTS AND DISCUSSIONS

To verify the performance, the proposed antenna was fabricated and measured. The top and side view of the prototype are shown in Fig.9. The modified half E-shaped patch is printed on the surface of the top FR4 substrate with a thickness of $h_0 = 1$mm. The NFRP patch on the top of the bottom FR4 substrate has a thickness of $h_0 = 1$mm. Four Teflon posts are used to assemble the fabricated antenna, whereas the ground plane and four rotated metallic plates are made of aluminum. It is apparent that the four metallic plates and the additional NFRP patch increase neither the footprint nor the height of the modified half E-shaped patch antenna. Hence, the proposed antenna has the characteristics of a compact and low profile structure. The N5247A network analyzer is used to measure the reflection coefficients of the antenna. The measurements of actual gain, AR, efficiency and radiation patterns were carried out with the Near Field Antenna Measurement System, Satimo.

Fig. 10(a) and Fig.10(b) show the simulated and measured reflection coefficients and AR of the prototype, respectively. The measured impedance bandwidth for $|S11| < -10$ dB is 833-960MHz (14.2%), in contrast to the simulated value of 839-964MHz (13.9%). The 3-dB AR bandwidth of the antenna was measured at 846–926MHz (9.0%), in contrast to the simulated value of 853-936MHz (9.3%), which falls within the impedance passband. Measurements agree very well with the simulations.

The measured gain, total effeciency and the radiation pattern of the antenna prototype are also quite consistent with the simulated results. In Fig.10(c), the measured gain is stable, with an average gain of 7.3dBic over the 3dB AR bandwidth. There is a slight difference between the simulated and measured realized gains, which could be due to inaccuracy of the dielectric constants of the substrate and imperfect fabrication. The simulated and measured total efficiency is larger than 88% within the 3dB AR bandwidth (Fig. 11).

TABLE 2. Comparisions between the proposed antenna and the previous literature.

Refs	Axial ratio Bandwidth (AR<3dB)	Overlapping Bandwidth (|S11|<-10dB, AR<3dB)	Gain (dBic)	Dimension Size	Aperture Efficiency	Gain Bandwidth (Gain>6.5dBic)
[16]	865-946MHz, 8.95%	8.95%	7.0	$0.60\lambda_0\times0.60\lambda_0\times0.114\lambda_0$	109.6%	/
[17]	901-930MHz, 3.17%	3.17%	7.0	$0.46\lambda_0\times0.46\lambda_0\times0.10\lambda_0$	190.5%	/
[18]	902-929MHz, 3.0%	3.0%	6.0	$0.46\lambda_0\times0.46\lambda_0\times0.10\lambda_0$	151.4%	/
[19]	1540-1620MHz, 5.0%	5.0%	6.5	$0.46\lambda_0\times0.46\lambda_0\times0.13\lambda_0$	156.3%	/
[21]	2420-2640MHz, 8.7%	8.7%	7.0	$0.76\lambda_0\times0.76\lambda_0\times0.116\lambda_0$	80.2%	12.2%
[22]	870–940 MHz, 7.7%	7.7%	7.0	$0.48\lambda_0\times0.48\lambda_0\times0.10\lambda_0$	171.2%	13.6%
[23]	2390-2560MHz, 6.94%	6.94%	~7.0	$0.65\lambda_0\times0.65\lambda_0\times0.066\lambda_0$	91.5%	/
This work	846-926MHz, 9.0%	9.0%	7.3	$0.45\lambda_0\times0.45\lambda_0\times0.074\lambda_0$	217.8%	15.0%

[a] λ_0 is the free-space wavelength at center frequency of operating band.

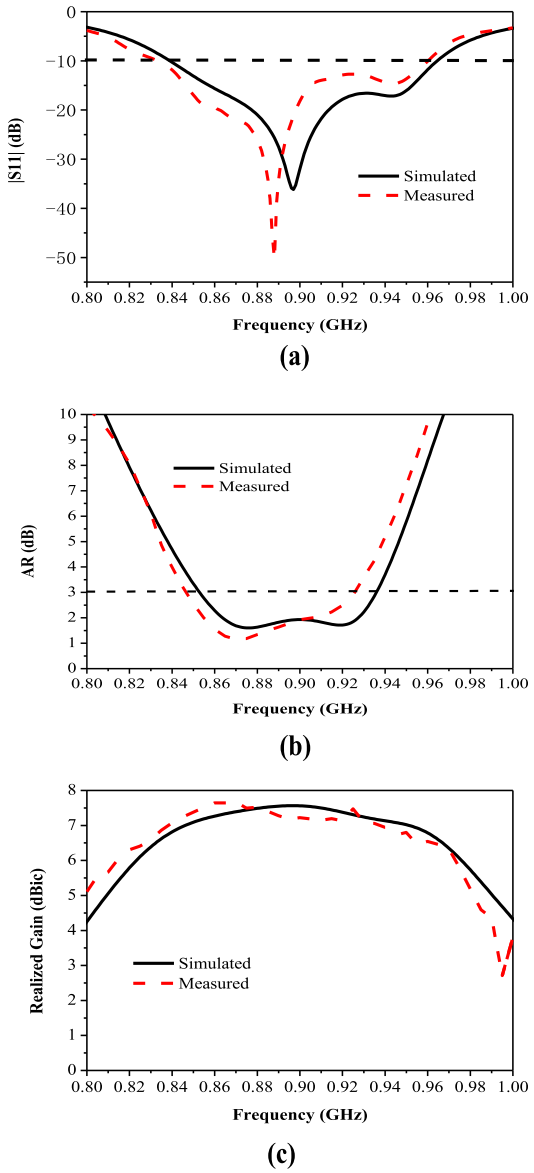

FIGURE 10. Simulated and measured results of: (a) reflection coefficients, (b) AR, and (c) realized gain.

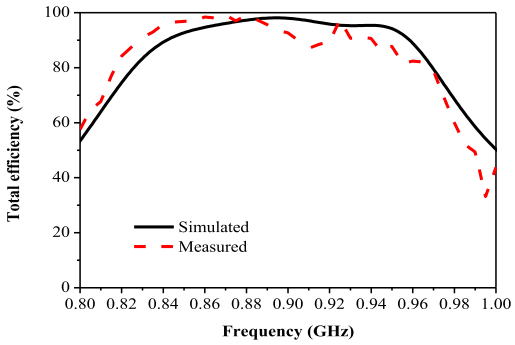

FIGURE 11. Simulated and measured total efficiency.

Fig. 12 and Fig. 13 show the simulated and measured radiation patterns in the X-Z and Y-Z planes of the proposed antenna at 870MHz and 920MHz, respectively. It is clearly seen that the antenna can generate stable broadside radiation patterns over the operating band. The measured half-power beamwidths are both approximately 77° at 870MHz and 920MHz. The cross-polarization (RHCP) is over 15 dB lower than the co-polarization (LHCP) in the boresight direction. Moreover, the measured front-to-back ratio can be as high as 15dB over the entire operational 3-dB AR bandwidth, which demonstrates that the measured antenna has a stable gain and low back radiation performance.

As mentioned above, the modified half E-shaped patch antenna with an elliptical slot and corner cut, NFRP patch, and four vertical rotated metal plates can improve impedance and AR bandwidth without increasing the total antenna height and footprint. Compared to the many single-feed CP antennas reported in the literature, our antenna has a wide AR bandwidth with a compact structure. A comprehensive comparison between previously-reported antennas and the proposed antenna is summarized in Table 2. As it has been shown that the L-shaped ground plane can increase the bandwidth [16], and the L-shaped probe technology can broaden the bandwidth [17], [18], however, these antennas are thicker than the present antenna. A stacked method was utilized in [19], [21]-[23] to increase impedance and CP bandwidth, but all dimensions were larger as a result. Notably, although the height of the antenna in [23] was slightly less than the proposed antenna, the AR bandwidth is narrower and a much lower aperture efficiency, limiting its scope of applications. In [17] the antenna has a large aperture efficiency but the

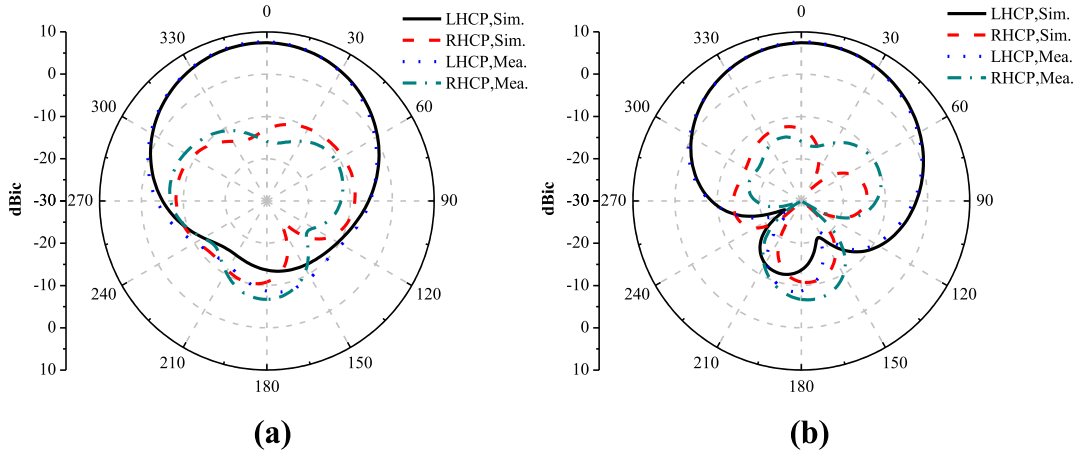

FIGURE 12. Measured and simulated radiation patterns at 870MHz in: (a) XOZ plane, (b) YOZ plane.

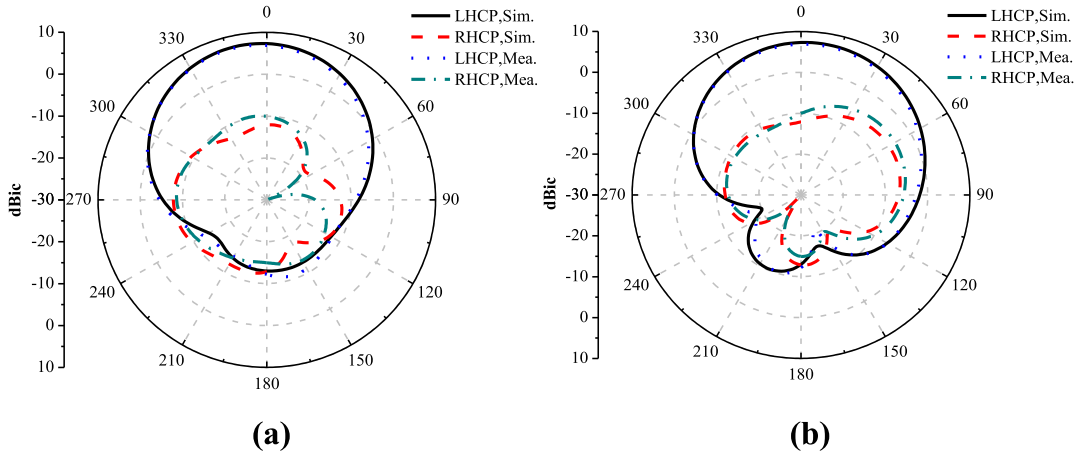

FIGURE 13. Measured and simulated radiation patterns at 920MHz in: (a) XOZ plane, (b) YOZ plane.

overlapping bandwidth is much narrower compared to the proposed antenna. For the proposed antenna, the measured minimal gain is 6.5dBic over the AR bandwidth and the relative bandwidth (with respect to the central frequency) for gain>6.5dBic is 15.0%. The gain bandwidths (gain >6.5dBic) in references [21] and [22] are smaller (12.2% and 13.6%, respectively) and have been added in Table 2 for comparison (gain bandwidths in other comparison references can not be found). The proposed antenna has a much larger aperture efficiency (217%) than those in all other relevant references. Furthermore, the measured front-to-back ratio of the proposed antenna ranged from 15.2 to 18.3dB over the entire operational 3-dB AR bandwidth, which is larger than e.g. the one in reference [22] (ranging from 9.15 to 12.15dB). Although front-to-back ratio of antenna in [23] is also larger than 15dB at center frequency of 2.45GHz, the antenna footprint is larger and the CP bandwidth is narrow. This indicates that our design method is much more suitable to enhance CP bandwidth and maintain a compact structure for RFID reader antennas, covering UHF RFID bands from 846 to 926MHz.

V. CONCLUSION

A wideband single-fed CP patch antenna with enhanced axial ratio bandwidth has been presented. The main features of the proposed antenna are the presence of four rotated metallic plates, and a main radiation patch etched with an elliptical slot and a corner cut. It has been found that the four vertical rotated metallic plates on the ground plane can decrease the size of the modified half E-shaped patch antenna. The resonant frequency of the modified half E-shaped patch antenna has decreased about 10% with the addition of the metallic plates. The elliptical slot and the corner cut on the modified half E-shaped patch adjust the impedance and CP performance of the antenna. Moreover, the introduction of the NFRP patch can improve the impedance and AR bandwidth without increasing the height of the antenna. The measured results (in good agreement with the corresponding simulated values) show that the proposed antenna has an impedance bandwidth ($|S11| < -10$dB) of 14.1% (833–960 MHz), a 3-dB AR bandwidth of 9.0% (846-926MHz), a stable gain of 7.3 dBic on average, and a front-to-back ratio over 15dB

(within the 3-dB AR band). The prototype can generate LHCP over the AR bandwidth. The proposed antenna is suitable for UHF RFID reader applications.

REFERENCES

[1] C. A. Balanis, "Microstrip antennas," in *Antenna Theory: Anal. Design*, 3rd ed. Hoboken, NJ, USA: Wiley, 2005, pp. 859–864.

[2] Z. N. Chen, X. Qing, and H. L. Chung, "A universal UHF RFID reader antenna," *IEEE Trans. Microw. Theory Techn.*, vol. 57, no. 5, pp. 1275–1282, May 2009.

[3] X. Liu, Y. Liu, and M. M. Tentzeris, "A novel circularly polarized antenna with coin-shaped patches and a ring-shaped strip for worldwide UHF RFID applications," *IEEE Antennas Wireless Propag. Lett.*, vol. 14, pp. 707–710, 2015.

[4] J. Zhuang, Y. Zhang, W. Hong, and Z. Hao, "A broadband circularly polarized patch antenna with improved axial ratio," *IEEE Antennas Wireless Propag. Lett.*, vol. 14, pp. 1180–1183, 2015.

[5] Q. Liu, J. Shen, H. Liu, Y. Wu, M. Su, and Y. Liu, "Low-cost compact circularly polarized directional antenna for universal UHF RFID handheld reader applications," *IEEE Antennas Wireless Propag. Lett.*, vol. 14, pp. 1326–1329, 2015.

[6] X. Chen, L. Wang, D. Wu, J. Lei, and G. Fu, "Compact and wideband directional circularly polarized distributed patch antenna with high efficiency," *IEEE Access*, vol. 5, pp. 15942–15947, 2017.

[7] Q. Liu, Y. Li, Z. Mo, and Y. Liu, "Compact broadband circularly-polarised directional universal GNSS antenna with symmetric radiation pattern and stable near-zenith coverage," *IET Microw. Antennas Propag.*, vol. 11, no. 5, pp. 657–663, Apr. 2017.

[8] K. L. Chung, Y. Li, and C. Zhang, "Broadband artistic antenna array composed of circularly-polarized Wang-shaped patch elements," *AEU-Int. J. Electron. Commun.*, vol. 74, pp. 116–122, Apr. 2017.

[9] Nasimuddin, Z. N. Chen, and X. Qing, "Asymmetric-circular shaped slotted microstrip antennas for circular polarization and RFID applications," *IEEE Trans. Antennas Propag.*, vol. 58, no. 12, pp. 3821–3828, Dec. 2010.

[10] N. Nasimuddin, X. Qing, and Z. N. Chen, "Compact asymmetric-slit microstrip antennas for circular polarization," *IEEE Trans. Antennas Propag.*, vol. 59, no. 1, pp. 285–288, Jan. 2011.

[11] Y.-F. Lin, C.-H. Lee, S.-C. Pan, and H.-M. Chen, "Proximity-fed circularly polarized slotted patch antenna for RFID handheld reader," *IEEE Trans. Antennas Propag.*, vol. 61, no. 10, pp. 5283–5286, Oct. 2013.

[12] A. Farswan, A. K. Gautam, B. K. Kanaujia, and K. Rambabu, "Design of Koch fractal circularly polarized antenna for handheld UHF RFID reader applications," *IEEE Trans. Antennas Propag.*, vol. 64, no. 2, pp. 771–775, Feb. 2016.

[13] K. Wei, J. Y. Li, L. Wang, R. Xu, and Z. J. Xing, "A new technique to design circularly polarized microstrip antenna by fractal defected ground structure," *IEEE Trans. Antennas Propag.*, vol. 65, no. 7, pp. 3721–3725, Jul. 2017.

[14] C. Y. D. Sim, Y. W. Hsu, and G. Yang, "Slits loaded circularly polarized universal UHF RFID reader antenna," *IEEE Antennas Wireless Propag. Lett.*, vol. 14, pp. 827–830, 2015.

[15] C. Y. D. Sim, Y. W. Hsu, C. W. Lin, and G. Yang, "Broadband circularly polarized antenna with moon-shaped parasitic element," *Int. J. RF Microw. Comput.-Aided Eng.*, vol. 26, no. 5, pp. 387–395, Feb. 2015.

[16] C. Y. D. Sim, C. C. Chen, R. Cao, and B. S. Chen, "A circular patch antenna with parasitic element for UHF RFID applications," *Int. J. RF Microw. Comput.-Aided Eng.*, vol. 25, no. 8, pp. 681–687, Oct. 2015.

[17] C. Y. D. Sim and C. J. Chi, "A slot loaded circularly polarized patch antenna for UHF RFID reader," *IEEE Trans. Antennas Propag.*, vol. 60, no. 10, pp. 4516–4521, Oct. 2012.

[18] C. H. Yeh, Y.-W. Hsu, and C. Y. D. Sim, "Equilateral triangular patch antenna for UHF RFID applications," *Int. J. RF Microw. Comput.-Aided Eng.*, vol. 24, no. 5, pp. 580–586, Mar. 2014.

[19] T. Mondal, S. Samanta, R. Ghatak, and S. R. B. Chaudhuri, "A novel hexagonal wideband circularly polarized stacked patch microstrip antenna," *Microw. Opt. Technol. Lett.*, vol. 57, no. 11, pp. 2548–2554, Nov. 2015.

[20] Nasimuddin, X. Qing, and Z. N. Chen, "A wideband circularly polarized stacked slotted microstrip patch antenna," *IEEE Antennas Propag. Mag.*, vol. 55, no. 6, pp. 84–99, Dec. 2013.

[21] T.-N. Chang, J.-M. Lin, and Y. G. Chen, "A circularly polarized ring-antenna fed by a serially coupled square slot-ring," *IEEE Trans. Antennas Propag.*, vol. 60, no. 2, pp. 1132–1135, Feb. 2012.

[22] T.-N. Chang and J.-M. Lin, "Circularly polarized ring-patch antenna," *IEEE Antennas Wireless Propag. Lett.*, vol. 11, pp. 26–29, 2012.

[23] C. Deng, X. Lv, and Z. Feng, "Low-profile circularly polarised patch–ring antenna with compact feeding network," *IET Microw. Antennas Propag.*, vol. 12, no. 3, pp. 410–415, Feb. 2018.

[24] K. L. Chung and A. S. Mohan, "A circularly polarized stacked electromagnetically coupled patch antenna," *IEEE Trans. Antennas Propag.*, vol. 52, no. 5, pp. 1365–1369, May 2004.

[25] K. L. Chung, "A wideband circularly polarized H-shaped patch antenna," *IEEE Trans. Antennas Propag.*, vol. 58, no. 10, pp. 3379–3383, Oct. 2010.

[26] Z. Wang, S. Fang, S. Fu, and S. Jia, "Single-fed broadband circularly polarized stacked patch antenna with horizontally meandered strip for universal UHF RFID applications," *IEEE Trans. Microw. Theory Techn.*, vol. 59, no. 4, pp. 1066–1073, Apr. 2011.

[27] C. Cho, H. Choo, and I. Park, "Broadband RFID tag antenna with quasi-isotropic radiation pattern," *Electron. Lett.*, vol. 41, no. 20, pp. 1091–1092, Sep. 2005.

[28] C. Cho, H. Choo, and I. Park, "Design of planar RFID tag antenna for metallic objects," *Electon. Lett.*, vol. 44, no. 3, pp. 175–177, Jan. 2008.

[29] J. M. Kovitz, H. Rajagopalan, and Y. Rahmat-Samii, "Circularly polarised half E-shaped patch antenna: A compact and fabrication-friendly design," *IET Microwaves, Antennas Propag.*, vol. 10, no. 9, pp. 932–938, 2016.

[30] Y. M. Pan, W. J. Yang, S. Y. Zheng, and P. F. Hu, "Design of wideband circularly polarized antenna using coupled rotated vertical metallic plates," *IEEE Trans. Antennas Propag.*, vol. 66, no. 1, pp. 42–49, Jan. 2018.

[31] R. Xu, J.-Y. Li, K. Wei, and G.-W. Yang, "A broadband slot antenna with unidirectional circularly polarized radiation patterns," *IEEE Antennas Wireless Propag. Lett.*, vol. 16, pp. 317–320, 2017.

[32] M.-C. Tang, X. Chen, M. Li, and R. W. Ziolkowski, "A bandwidth-enhanced, compact, single-feed, low-profile, multilayered, circularly polarized patch antenna," *IEEE Antennas Wireless Propag. Lett.*, vol. 16, pp. 2258–2261, 2017.

JUNLONG LI was born in Guangdong, China, in 1992. He received the B.S. degree in electronic and information engineering from the University of Electronic Science and Technology of China, Zhongshan Institute, Zhongshan, China, in 2016. He is currently pursuing the M.E. degree in electromagnetic field and microwave technology from the Centre for Optical and Electromagnetic Research, Academy of advanced Optoelectronics, South China Normal University, Guangzhou, China. His current research interests include RF circuits, circularly polarized antennas, and antenna miniaturization.

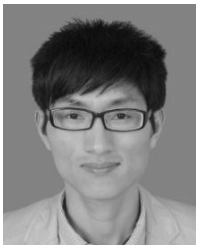

HUI LIU was born in Henan, China. He received the M.S. degree in electromagnetic field and microwave technology and the Ph.D. degree in microelectronics and solid state electronics from the Centre for Optical and Electromagnetic Research, Academy of Advanced Optoelectronics, South China Normal University, Guangzhou, China, in 2013 and 2018, respectively. Since 2018, he has been a Post-Doctoral Fellow with the Centre for Optical and Electromagnetic Research, Zhejiang University, Zhejiang, China. His research interests include antenna, RF circuit, and microwave component.

SHUAI ZHANG was born in Liaoning, China, in 1983. He received the B.E. degree from the University of Electronic Science and Technology of China, Chengdu, China, in 2007, and the Ph.D. degree in electromagnetic engineering from the Royal Institute of Technology (KTH), Stockholm, Sweden, in 2013. After his Ph.D. studies, he was a Research Fellow at KTH. In 2010 and 2011, he was a Visiting Researcher with Lund University, Sweden, and with Sony Mobile Communications AB, Sweden, respectively. In 2014, he joined Aalborg University, Denmark, where he is currently an Associate Professor. He is also an External Antenna Specialist at Bang & Olufsen, Denmark. His research interests include mobile terminal mmwave antennas, biological effects, nanosatellite antennas, UWB wind turbine blade deflection sensing, MIMO antenna systems, and RFID antennas.

MIAOHUI LUO was born in Guangdong, China, in 1992. He received the B.S. degree in information engineering from South China Normal University, Guangzhou, China, in 2016, where he is currently pursuing the M.E. degree in optics from the Centre for Optical and Electromagnetic Research, Academy of Advanced Optoelectronics. He current research interests include retrodirective antenna and UWB antenna.

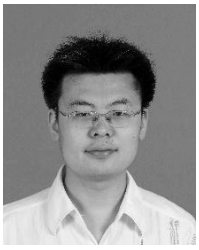

YUAN ZHANG was born in Shanxi, China, in 1980. He received the bachelor's degree and the Ph.D. degree in optical engineering from the Beijing institute of Technology, Beijing, China, in 2003 and 2009, respectively. He moved to Nanyang Technological University, Singapore, in 2009, and Zhejiang University, Zhejiang, China, in 2010, as a Post-Doctoral Fellow. Since 2014, he has been a Faculty Member with the Centre for Optical and Electromagnetic Research, South China Normal University, Guangzhou, China. His research focuses on metamaterials and artificial electromagnetic structures with interesting properties.

SAILING HE (M'92–SM'98–F'13) was born in Zhejiang, China, in 1966. He received the Licentiate of Technology degree and the Ph.D. degree in electromagnetic theory from the Royal Institute of Technology (KTH), Stockholm, Sweden, in 1991 and 1992, respectively. Since 1992, he has been with the Royal Institute of Technology as an Assistant Professor, an Associate Professor, and a Full Professor. He is also with Zhejiang University (ZJU) as a Distinguished Professor of a special program, as well as a Joint Research Center between KTH and ZJU. He has first authored one monograph and authored/co-authored about 400 papers in refereed international journals. His current research interests include electromagnetic metamaterials, optoelectronics, microwave photonics, and biomedical applications. He has given many invited/plenary talks in international conferences, and has served in the leadership for many international conferences. He is a fellow of the Optical Society of America, the International Society for Optical Engineering, and the EM Academy.